Muon spin relaxation study of non-Fermi-liquid behavior near the ferromagnetic quantum critical point in $CePd_{0.15}Rh_{0.85}$

D. T. Adroja,[1,*] A. D. Hillier,[1] J.-G. Park,[2] W. Kockelmann,[1] K. A. McEwen,[3] B. D. Rainford,[4] Kwang-Hyun Jang,[2] C. Geibel,[5] and T. Takabatake[6]

[1]*ISIS Facility, STFC Rutherford Appleton Laboratory, Chilton, Didcot, Oxfordshire, OX11 0QX, United Kingdom*

[2]*Department of Physics, SungKyunKwan University, Suwon 440-746, Republic of Korea and Center for Strongly Correlated Materials Research, Seoul National University, Seoul 151-747, Republic of Korea*

[3]*Department of Physics and Astronomy, and London Centre for Nanotechnology, University College London, Gower Street, London WC1E 6BT, United Kingdom*

[4]*Department of Physics and Astronomy, Southampton University, Southampton, SO17 0BJ, United Kingdom*

[5]*Max-Planck Institute for Chemical Physics of Solids, D-01187 Dresden, Germany*

[6]*Department of Quantum Matter, ADSM, Hiroshima University, Higashi-Hiroshima, 739-8530, Japan*

(Received 4 February 2008; published 8 July 2008)

The low-energy spin dynamics near the ferromagnetic quantum critical point in $CePd_{0.15}Rh_{0.85}$ have been investigated using zero-field (ZF) and longitudinal-field muon spin relaxation (μSR) measurements over a temperature range of 60 mK to 4 K and in applied fields up to 2500 G. The ZF-μSR measurements reveal a considerable slowing down of the spin fluctuations with decreasing temperatures below 2 K. There is no clear sign of either static long-range magnetic ordering or spin freezing down to 60 mK. The temperature dependence of the ZF-muon depolarization rate (λ) exhibits a power-law behavior, $\lambda(T) \sim T^{-n}$ with $n \sim 0.8$, while the field dependence at 0.1 K reveals a time-field scaling of the muon relaxation function, $P_z(t,H) = P_z(t/H^{\gamma})$ with $\gamma \sim 1.0 \pm 0.1$. Furthermore, the exponent derived from the ZF-μSR data agrees well with the power-law behavior of the temperature-dependent susceptibility, $\chi(T) \sim T^{-\alpha}$ ($\alpha \sim -0.6 \pm 0.1$), the E/T scaling of the neutron dynamical susceptibility, as well as the magnetization-field-temperature scaling ($\gamma_m \sim 0.8 \pm 0.1$), obtained from the same sample. The μSR results of $CePd_{0.15}Rh_{0.85}$ are discussed in the context of systems exhibiting non-Fermi-liquid behavior.

DOI: 10.1103/PhysRevB.78.014412 PACS number(s): 75.30.−m, 71.27.+a, 75.40.Cx

I. INTRODUCTION

One of the most fascinating areas in condensed-matter physics today is the investigation of metals in which the correlations among conduction electrons are strongly enhanced. Ever since its inception, Landau's Fermi-liquid theory has been the fundamental foundation for our understanding of the low-temperature properties of these strongly correlated electron systems,[1] which incorporate the effect of electronic interactions into a renormalized electron mass. Recently, however, the breakdown of Fermi-liquid theory has been observed in several strongly correlated f-electron materials: the so-called non-Fermi-liquid (NFL) behavior.[2–5] This breakdown has far-reaching implications on our current understanding of metals. One good example is the normal state of high-temperature superconductors,[4] which exhibit linear resistivity above T_c up to 1000 K. These unusual systems display such NFL behavior when their ordered magnetic moments are forced to quench with their second-order phase transitions, suppressed to $T \rightarrow 0$ K by external parameters such as pressure, magnetic fields, and doping. These are also sometimes called zero-temperature quantum phase transitions or quantum critical points (QCP).[2–4] It is to be noted that QCP is one of the mechanisms for NFL behavior; however, there are various other mechanisms for NFL behavior, which are discussed below.

When such a quantum phase transition occurs, the low-temperature magnetic, transport, and thermal properties of such compounds differ significantly from those of simple metals, and from some magnetically ordered heavy-fermion compounds, whose properties are usually understood within the formalism of Fermi-liquid theory. The most striking and general features of a material at a quantum-phase transition are (i) the linear temperature (T) dependence of the electrical resistivity, (ii) the logarithmic temperature dependence of the electronic specific-heat coefficient C/T, and (iii) the power-law or square-root temperature dependence of the magnetic susceptibility.[2–5] These electronic properties are entirely different from those expected from the Fermi-liquid theory for simple metals and magnetic heavy-fermion compounds. Therefore, the anomalous magnetic, thermal, and transport properties of materials near a quantum-phase transition are described as non-Fermi-liquid behavior.[2–5] Several scenarios of non-Fermi-liquid behavior have been suggested theoretically.[2,6–13] Some of the most actively discussed theoretical explanations include a model based on disorder effects such as the Kondo disorder model and Griffiths phase scenarios,[10,11] a model based on spin-density wave scenarios with a Gaussian fixed point now known as a nonlocal QCP (Refs. 6–8), and a model based on a non-Gaussian fixed point and having second-order quantum phase transitions known as a local QCP.[12,13]

So far most of the NFL systems investigated in the field of strongly correlated electron systems deal with a vanishing *antiferromagnetic* phase transition at $T=0$ K, which are denoted as an antiferromagnetic quantum critical point (AFQCP). From a materials' point of view, it is noticeable that there are only a handful of systems that show clear evi-

dence of NFL behavior near a *ferromagnetic* quantum critical point (FQCP).[14–16] The FQCP is expected to be very different from the AFQCP in many respects.[17–20] Some of the key differences are as follows: (1) it is intrinsically a $q=0$ phase transition, hence, order parameters are conserved. (2) In the quasiclassical regime of an FQCP, the dynamic spin fluctuations enhance the Kondo temperature, T_K. (3) The dynamical critical exponent z_d is three, whereas z_d is two for an AFQCP. (4) Approaching the QCP from the high-temperature side, the magnetic correlation length (ξ) diverges as $T^{-2/3}$ unlike as $T^{-3/4}$ (in Hertz-Millis theory) for an AFQCP.[6,8] More interestingly, recent theoretical studies of emergent superconductivity in electronic systems close to a FQCP show that the system avoids pair breaking effects by undergoing a first-order transition with a much larger T_{sc} near FQCP,[19,20] which agrees with experimental observations in UGe_2 and URhGe.[21,22] A similar weak first-order transition from FM Fermi-liquid to nonmagnetic non-Fermi-liquid behavior in the resistivity has been observed near the FCQP under applied pressure in MnSi.[23]

In this respect, it is interesting to note that recent bulk measurements have shown that $CePd_{1-x}Rh_x$ alloys exhibit NFL behavior near a FQCP for the critical composition $x_c=0.85$.[24–26] CeRh shows mixed-valence behavior with strong hybridization between $4f$ and conduction electrons while CePd exhibits ferromagnetic ordering with $T_C=6$ K. It has been shown by Sereni and co-workers[24–26] that, in $CePd_{1-x}Rh_x$, a continuous decrease of the ferromagnetic ordering temperature T_C with increasing x takes place down to $T_C=0.25$ K at $x=0.80$. This suggests that in $CePd_{1-x}Rh_x$ the ferromagnetic order disappears at a quantum critical point placed around $x_c=0.85$.[24,25] It should be noted that the recent work of Sereni *et al.*[26] indicates that the critical composition lies between $x_c=0.87$ and 0.90. However, our muon spin relaxation (μSR) experiment shows that our sample, with $x=0.85$, is on or very close to the critical composition. More interestingly, the unit-cell volume exhibits a linear behavior with increasing Rh concentrations for $0<x<0.75$ and then exhibits a change in the slope for $0.75<x<1.0$.[26] This then indicates that there is a certain valence instability before the critical composition $x_c=0.85$, at which composition experimental evidence is found of a FQCP. It is to be noted that this behavior is very different from that observed in many other QCP/NFL systems, where the Ce valence remains nearly trivalent, e.g., $Ce(Cu,Au)_6$ and $CeRh_2Ga$.[27,28] Recently, we have investigated the spin dynamics and E/T scaling near the FQCP in $CePd_{0.15}Rh_{0.85}$ using inelastic neutron-scattering (INS) measurements.[29] Since muon spin relaxation and INS measurements are complementary tools, they provide, when used together, a wealth of information about the microscopic magnetic interactions. We have now carried out μSR measurements on this compound in order to further our understanding of the ground state as well as the nature of low-energy spin fluctuations in $CePd_{0.15}Rh_{0.85}$. Our zero-field μSR study clearly shows the slowing down of the spin-fluctuation rate and the power-law divergence of the μSR depolarization rate (λ) at low temperatures without any clear sign of long-range magnetic ordering down to 60 mK.

II. EXPERIMENT DETAILS

The polycrystalline sample of $CePd_{0.15}Rh_{0.85}$ was prepared by arc melting the constituent elements with purity of 99.9% at SungKyunKwan University, South Korea. In order to ensure homogeneity, the button was flipped over and remelted several times. The sample was annealed at 700 °C for a week in a sealed quartz tube. The phase purity of the sample was checked by neutron powder-diffraction measurements using the GEM diffractometer at the ISIS pulsed neutron and muon facility, U.K. The temperature dependence of the bulk magnetic susceptibility and magnetization isotherms was measured using a commercial Quantum Design PPMS magnetometer. The μ^+SR measurements were performed using the MuSR spectrometer at ISIS, where a pulse of muons is produced every 20 ms and has a full width at half maximum of 70 ns. These muons are implanted into the sample, after which they decay with a half life of 2.2 μs into positrons, which are emitted preferentially in the direction of the muon spin axis. These positrons are detected and time stamped in the detectors that are positioned before (F) and after (B) the sample. The muon relaxation function $P_z(t)$ was obtained, using the counts in F and B detectors, as $P_z(t)=N_F(t)-\alpha N_B(t)/N_F(t)+\alpha N_B(t)$, where α is a calibration constant. $P_z(t)$ provides information about the internal field and the spin-lattice relaxation rate. We have carried out zero-field (ZF) and longitudinal-field (LF) μSR measurements, in applied fields up to 2500 G, over the temperature range from 60 mK to 4 K. The powder sample was fixed to a silver backing plate and mounted onto the cold finger of a dilution refrigerator. The silver sample holder was used because it gives a nonrelaxing muon signal, and hence, only contributes a temperature-independent constant background.

III. RESULTS AND DISCUSSION

A. Neutron diffraction

Figure 1 shows a neutron-diffraction pattern from the $CePd_{0.15}Rh_{0.85}$ powder sample obtained on GEM at 300 K. The sharpness of the linewidths of the peaks suggests that the sample is well crystallized and homogeneous. Rietveld analysis of the neutron-diffraction data, using the GSAS program, confirmed that the $CePd_{0.15}Rh_{0.85}$ sample is single-phase, and crystallizes in the orthorhombic CrB-type structure (Fig. 2) with space-group Cmcm (No 63) and four molecular formula units per unit cell. In this structure, the Ce and Rh (Pd) atoms each occupy a special and unique crystallographic site. The Ce atom was assigned to the "4c" (0, y_{Ce}, $1/4$) crystallographic site and the Rh (Pd) atom to the 4c (0, y_{Rh}, $1/4$) crystallographic site. The refined values of the orthorhombic lattice parameters are $a=3.8801(8)$, $b=10.9666(3)$, and $c=4.2381(1)$ Å; the refined value of the unit-cell volume is 180.338 Å^3, which is in good agreement with the reported value in Ref. 26. The atomic position parameters of the Ce and Rh(Pd) atoms are $y_{Ce}=0.1376(1)$ and $y_{Rh}=0.4091(1)$. Isotropic thermal factors were also refined, and found to be 0.0075(2) Å^2 for Ce and 0.0176(3) Å^2 for Rh (Pd), respectively, while keeping the site occupancy fixed to 100%. The best fit gave a weighted profile R value of R_W

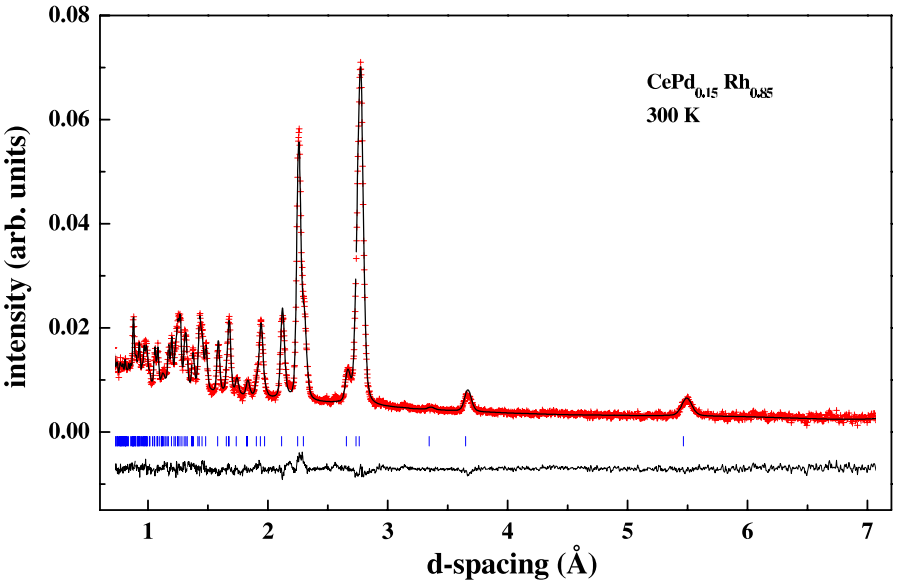

FIG. 1. (Color online) Neutron diffraction pattern of $CePd_{0.15}Rh_{0.85}$ obtained on GEM at ISIS at ambient temperatures. The symbols show the data, the line represents the Rietveld fit, and the vertical bars denote symmetry-allowed peak positions. The difference between the calculation and observed counts is shown as a solid line at the bottom of the plots.

of 4.8% as average for the six GEM banks. The quality of the fit can be seen in Fig. 1 for one of the GEM detector banks. The calculated bond distances from the refined parameters are as following: Ce-4Rh(Pd)=2.9192(1), Ce-Rh =2.9770(9), Ce-2Rh=3.1703(7), Ce-4Ce=3.7864(7), Ce-2Ce=3.6877(9), and Ce-2Ce=3.8830(8), all in units of angstrom. It is to be noted that the shortest bond-distance between Ce-4Rh is most likely an important parameter for the observed strong hybridization between Ce-4f and Rh-4d electrons, and hence, the mixed-valence nature of the Ce ion in $CePd_{1-x}Rh_x$ for $x=0.7-1.0$.

B. Magnetic susceptibility and magnetization

Figure 3 shows the magnetic and inverse magnetic susceptibilities measured in an applied field of 0.5 T between 2 and 300 K. The susceptibility exhibits a large enhancement at low temperatures over the Curie-Weiss susceptibility of the Ce^{3+} ion, which is in agreement with the previous reported behavior.[25,26] The low-temperature susceptibility, when plotted on a log-log scale, exhibits a power-law divergence $\chi(T)\sim T^{-\alpha}$ with $\alpha=0.6\pm0.1$, which has been attributed to NFL behavior.[25,26] Concerning the power-law behavior, we note that the value of the exponent α observed here is identical to the exponent $\sim$0.6 observed in the E/T scaling of the dynamical susceptibility of $CePd_{0.15}Rh_{0.85}$.[29] The spin-fluctuation theories of Moriya and Lonzarich[7] predict the value of the exponent $n=4/3$ for a three-dimensional (3D) ferromagnetic quantum critical point, compared with $\alpha=3/2$ for a 3D antiferromagnetic quantum critical point:[2,7] for the two-dimensional (2D) FM case, $\alpha=1$ is predicted by the theory of Lonzarich[2,7] while $\chi(T)\sim T^{-1}/\log T$ behavior is predicted by the theory of Moriya.[2,7] Thus the observed temperature dependence of the susceptibility at low temperatures does not agree with the predictions of the NFL spin-fluctuation theories based on 3D and 2D FM. However, the value of the observed exponent is close to the prediction $\alpha=3/4$ for the disorder Kondo alloy model for NFL behavior by Grempel and Rozenberg.[30] We recall that NFL systems such as $YbRh_2(Si_{1-x}Ge_x)_2$ and $CeNi_{0.55}Co_{0.45}Sn$ also exhibit a power-law divergence in the susceptibility with $\alpha\sim0.6$.[31,32] For the former compound, it has been shown that both ferromagnetic and antiferromagnetic fluctuations are important for explaining the observed NFL behavior[33] while the latter system exhibits NFL behavior when the first-order valence phase transition, observed for $CeNi_{0.65}Co_{0.35}Sn$, is suppressed by further increasing the Co composition. Interestingly, the power-law divergence in the susceptibility was also observed in $Ce_{1-x}Th_xRhSb$ ($x=0.1-0.3$) with $\alpha=0.36-0.44$, whose origin was attributed to a Griffith phase model.[2]

The presence of strong Kondo-type interactions in $CePd_{0.15}Rh_{0.85}$ can be seen from the high value of the Curie-Weiss (CW) temperature, $\theta_P=-184$ K, obtained from the CW behavior of the high-temperature susceptibility. Despite $CePd_{0.15}Rh_{0.85}$ being close to a FQCP, θ_P is very large and

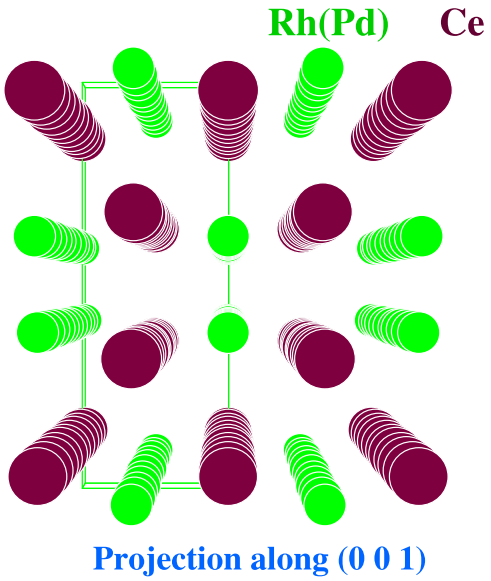

FIG. 2. (Color online) CrB-type orthorhombic unit cell of $CePd_{0.15}Rh_{0.85}$ with space-group Cmcm.

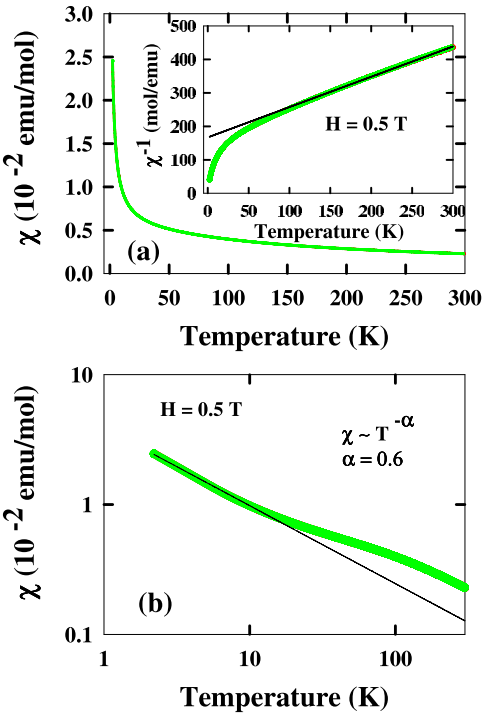

FIG. 3. (Color online) (a) Temperature dependencies of the magnetic susceptibility and the inverse magnetic susceptibility of $CePd_{0.15}Rh_{0.85}$. (b) Log-log plot of the temperature dependence of the magnetic susceptibility. The solid straight line in (a) indicates Curie-Weiss behavior while in (b) the line demonstrates a power-law behavior.

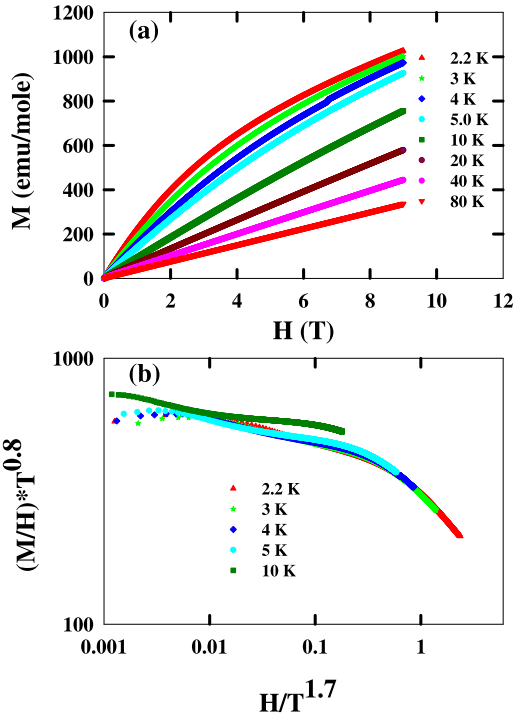

FIG. 4. (Color online) (a) Magnetization isotherms of $CePd_{0.15}Rh_{0.85}$ at temperatures between 2.2 and 80 K. (b) Scaling of $M(H,T)$ plotted as $\log \log(M/H)T^{0.8}$ versus $\log(H/T^{1.7})$ of the data between 2.2 and 10 K.

negative rather than small and positive, as might be expected for a system near a FQCP. There are two possible explanations for the observed large value of θ_P: (i) the crystal electric-field (CEF) effect, and (ii) strong hybridization between $4f$ and conduction electrons. However, we failed to observe well-defined CEF excitations in our high energy inelastic neutron-scattering experiments. Instead, a broad magnetic excitation extending up to 60 meV was observed. This then can be interpreted that the origin of the large negative value of θ_P is most likely to be due to the presence of strong hybridization, which yields a high Kondo temperature. Furthermore, it should be noted that low-energy inelastic neutron scattering also reveals clear quasielastic signals that exhibit E/T scaling.[29] This is in contrast with other well-known mixed-valence systems where one observes only inelastic scattering and no clear presence of quasielastic scattering, e.g., in $CePd_3$ and $CeRu_4Sb_{12}$.[34,35] In this case, the position of the inelastic peak can be taken as a good measure of T_K for these systems.[35] This further indicates that the $CePd_{0.15}Rh_{0.85}$ system contains some Ce ions with a small Kondo temperature. From this we may infer that $CePd_{0.15}Rh_{0.85}$ has a distribution of Kondo temperatures with a finite value of the distribution function $P(T_K=0)$ at $T_K=0$.[10] Thus the uncompensated moment with $T_K=0$ may be responsible for the observed non-Fermi-liquid behavior at low temperatures. On the other hand, we note that a model proposed by Bernhoeft[36] is based on the distribution of the relaxation rates having lower and upper bounds.

Now let us discuss the isothermal magnetization measurements and their scaling properties. It was predicted theoretically by Tsvelik and co-workers[37,38] that NFL systems should exhibit scaling behavior in magnetization isotherms at various temperatures, i.e., $M(H,T)$. This model implies that the alloys have a critical point at $T=0$ and therefore their low-temperature thermodynamic properties are governed not by single-particle fermion excitations, as in the FL, but by the collective quantum fluctuations of the order parameter in the vicinity of the critical point. This scaling analysis is an extension of the scaling formalism in the Landau model, which describes critical behavior near a finite temperature second-order phase transition at the ordering temperature. According to Tsvelik *et al.*,[37] the functional form of the magnetization scaling is given as follows:

$$\frac{M}{H} = T^{-\gamma_m} f\left(\frac{H}{T^{(\beta_m+\gamma_m)}}\right). \quad (1)$$

Here subscript "m' indicates that these exponents are for the magnetization and should not be confused with the ones used in the muon relaxation function. The prediction of magnetization scaling has been previously observed in many NFL systems such as $U_{0.2}Y_{0.8}Pd_3$ (Ref. 38) and $U(Cu,Pd)_5$ (Ref. 39). We have therefore carried out magnetization measurements at various temperatures in order to check this scaling behavior. Figure 4(a) provides the summary of the magnetization data taken at various temperatures between 2.2 and 80 K in magnetic fields up to 9 T. As one can clearly see in the figure, the magnetization displays nonlinear behavior with field at low temperatures and then exhibits linear behavior at high temperatures. It is to be noted that the value of the

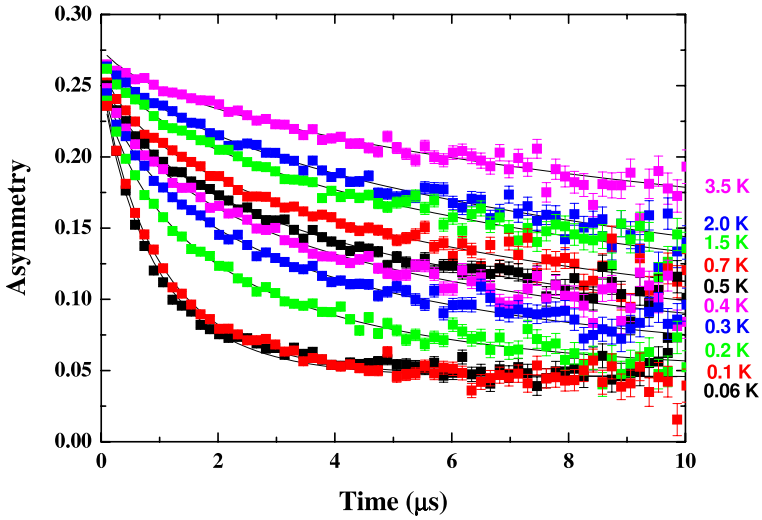

FIG. 5. (Color online) ZF-μSR spectra at selected temperatures between 60 mK and 4 K.

magnetic moment at 2.2 K and 9 T field is $0.2\mu_B$, which is much smaller than the free Ce^{3+} ion value of $2.54\mu_B$. In order to check the scaling of $M(H,T)$, we have also plotted the data in Fig. 4(b) as $(M/H)^* T^{\gamma m}$ versus $H/T^{\beta m+\gamma m}$ in a log-log plot. The values of γ_m and $\beta_m+\gamma_m$ were varied in order to find out the best fitting results of these parameters. From an extensive search of the parameter space, it was found that the values of $\gamma_m=0.8\pm0.1$ and $\beta_m+\gamma_m=1.7\pm0.1$ (i.e., $\beta_m=0.9$) give the best scaling behavior where all the data below 10 K collapse onto a universal curve, while data at 10 K and above (not shown in the plot) deviate considerably from the scaling curve. It should be noted that similar scaling behavior has been previously observed up to 10 K for $U_{0.2}Y_{0.8}Pd_3$ with $\gamma_m=0.3$ and $\beta_m=1.3$ while for $U(Cu,Pd)_5$, $\gamma_m=0.25$ and $\beta_m=1.2$.[38,39] For $CePd_{0.15}Rh_{0.85}$, the value of β_m is similar; however, the value of γ_m, which is also nearly the same as the observed exponent in the susceptibility, is twice that observed in the uranium systems. The large value of the exponents $(\beta_m+\gamma_m)$ indicates that the extended correlated fluctuations could be responsible for the singular behavior of $\chi\rightarrow0$.[2] We stress that for a true FL system, no such scaling behavior should be observable. The presence of $M(H,T)$ scaling indicates that there is an energy scale other than the Fermi energy that dominates the thermodynamic properties of NFL systems. We will compare this value of γ_m with the exponent obtained from the temperature dependence of the ZF-muon spin relaxation rate presented in the next section.

C. μSR measurements

1. Zero-field μSR measurements

Figure 5 shows the time dependence of the ZF-μSR relaxation function, $P_z(t)$, of $CePd_{0.15}Rh_{0.85}$ at various temperatures between 60 mK and 4 K. Down to the lowest measured temperature, we have observed neither any clear sign of loss of initial asymmetry (A_0) nor a clear signature of frequency oscillations. The absence of both features clearly rules out any possible static long-range magnetic ordering. Interestingly, with decreasing temperatures from 4 K, the relaxation rate increases and the signal is strongly damped below 1 K, which might indicate further slowing down of the spin-fluctuation rate at low temperatures.

To obtain quantitative information on the temperature dependence of the muon relaxation rate and line shape, we have analyzed the ZF spectra using the relaxation function of a stretched exponential form given as follows:

$$P_z(t) = A_0^* \exp[-(\lambda t)^\beta] + A_{bg}, \tag{2}$$

where A_{bg} is a background term arising from muons stopped in the silver sample holder and the first term is a rapidly damped contribution arising from the muons stopped in the bulk of the sample. Here λ is the damping rate and β is an exponent. It is to be noted that Eq. (2) interpolates between Gaussian line shape (when $\beta=2$) and Lorentzian line shape (when $\beta=1$). While pure Lorentzian or Gaussian functions provided no good fits to the data over the entire temperature range, the parameter β in Eq. (2) gives a crude indication of the behavior of the relaxation, i.e., whether the relaxation is dynamic $(\beta=1)$, static $(\beta=2)$, or intermediate. The stretched exponential form of the relaxation has also been used to fit the ZF- and LF-field μSR data of many NFL systems such as $U(Cu,Pd)_5$, $CePtSi_{1-x}Ge_x$, $YbRh_2Si_2$, and $CeNi_9Ge_4$,[40–43] but the Lorentzian form has been used for $CeRu_4Sn_6$ and $CeRu_4Sb_{12}$.[44,45] The detailed discussion on the underlying physics for various values of β can be found in Refs. 46 and 47. For the whole analysis, we kept the background term $A_{bg}=0.0456$ fixed. We note that our fit to the data at 4 K to Eq. (2) was very good, indicating that there is no significant contribution arising from the nuclear moments of either Rh or Pd, which would have given a static Kubo-Toyabe (KT) type line shape. The absence of a KT type relaxation rate may indicate that the muon stopping site in $CePd_{0.15}Rh_{0.85}$ is close to the Ce atoms, which do not have nuclear moments, and hence, do not contribute any KT-type damping. Furthermore, the use of a single component indicates that there is only one muon site, unlike the two sites observed in $CeCoGe_{1-x}Si_x$ $(x=1.2$ and $1.5)$ that also exhibits NFL behavior.[48] The values of the parameters λ and β, estimated from our analysis are plotted in Fig. 6 as a function of temperature. It is seen from Fig. 6(a) that when decreasing the

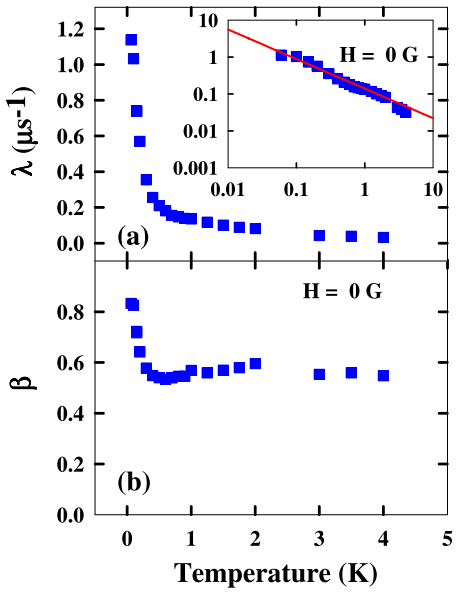

FIG. 6. (Color online) (a) Temperature dependence of the depolarization rate (λ) and (b) temperature dependence of the exponent (β) for the ZF-μSR data. The inset shows the log-log plot for the depolarization rate for the ZF data.

temperature from 4 to 1 K, λ first increases gradually but then exhibits a sharp rise below 1 K. Furthermore, a log-log plot [see the inset of Fig. 6(a)] exhibits a power-law type behavior with $\lambda(T) \sim 0.14\ T^{-0.8}$. This value of the exponent is reasonably close to 0.6–0.8, obtained from the temperature dependence of the susceptibility, E/T scaling of the dynamical susceptibility, and magnetization scaling, as mentioned previously. Furthermore, it is to be noted that the value of β (~0.6) is nearly temperature independent between 4 and 1 K before it increases and approaches one at the lowest temperature [Fig. 6(b)]. The rise may indicate that the relaxation function at the lowest temperature is close to a Lorentzian form. Further confirmation of the temperature dependence of β at low temperatures (below 0.4 K) is obtained with a data plot in the form of $P_z(t)$ versus $t^{1/2}$ (not shown here). The data above 0.3 K exhibited linear behavior but the data below 0.3 K displayed a noticeable deviation from a linear dependence above a time of 2.25 μs, indicating the previously mentioned change of the β value.

We comment that β=0.5 is to be expected for a rapidly fluctuating dynamic local Lorentzian field distribution arising from fluctuating atomic dipoles[49] above the spin-glass temperature (T_g) for dilute spin-glass systems while β=1/3 is expected for a concentrated spin-glass system at the spin freezing temperature.[49,50] The case of β=1/3 at T_g has been observed for the spin-glass systems such as $Y(Mn_{0.9}Al_{0.1})_2$ and AgMn (0.5 at %).[50,51] The case of β=1/2 has been found for $Y_6(Mn_{0.55}Fe_{0.45})_{23}$,[52] which does not show any sign of a long-range magnetic ordering but exhibits dynamic spin fluctuations, and for AuFe (1 at %),[53] which exhibits spin-glass-type behavior below 9.1 K. The observed temperature dependence of β for $CePd_{0.15}Rh_{0.85}$ at the lowest temperatures may rule out the possibility of a diluted or concentrated spin-glass system up to 60 mK and even at $T \to 0$. On the other hand, β=0.7 at lowest temperature of 0.05 K can be taken as an indication of a broad distribution of relaxation rates, as discussed for similar features found in UCu_4Pd.[40]

It is useful to compare the power-law behavior observed in ZF $\lambda(T)$ with a similar feature seen in the temperature dependence of the susceptibility $\lambda(T)$. For example, the temperature dependence of $\lambda(T)$ can be directly compared with the neutron-scattering linewidths via the formalism described by Lovesey *et al.*[54] Moreover, there exists a direct relationship between λ, the inelastic linewidth $\Gamma(q)$, and the wave vector dependent susceptibility $\chi(q)$:

$$\lambda = \left(\frac{BT}{N}\right)\sum_q \frac{\chi(q)}{\Gamma(q)}, \tag{3}$$

with

$$\frac{1}{N}\sum_q \chi(q) = \chi_L, \tag{4}$$

where $\chi(q)$ is related to the neutron dynamical susceptibility through a Kramers-Kronig relation,[55] χ_L is the local susceptibility, and B is the coupling constant. We have measured the inelastic neutron response of $CePd_{0.15}Rh_{0.85}$, which shows a q-independent behavior.[29] Furthermore, the temperature-dependent linewidth at low temperatures exhibits nearly linear behavior with temperature, $\Gamma(T) \propto T$. In a theoretical model of NFL behavior by Bernhoeft,[36] the low-energy linewidth also exhibits linear behavior with temperature while the high energy linewidth is temperature independent. Thus we can safely assume a linear behavior of $\Gamma(T)$ with temperature. If we take the observed power-law behavior in Fig. 3 as the temperature-dependent behavior of $\chi_L(T)$ at low temperatures, i.e., $\chi_L(T)\ \alpha\ T^{-\alpha}$, and substitute this form of $\Gamma(T)$ and $\chi_L(T)$ in Eq. (3), then the temperature dependence of $\lambda(T)$ becomes

$$\lambda(T) = BT^{-\alpha}. \tag{5}$$

Using this equation one can obtain a similar value of the exponent as observed in the temperature dependence of the ZF-muon relaxation rate of $CePd_{0.15}Rh_{0.85}$.

2. *Longitudinal field* μSR *measurements*

In order to study further the role of static and dynamic local internal fields as well as to investigate the time-field scaling,[40,41] we have carried out μSR measurements in applied longitudinal fields between 0 and 2500 G at 0.1 K. In longitudinal fields the muon spin relaxation is mainly due to thermally excited 4f-electron-spin fluctuations, which couple to the muons implanted in the sample. These muons at a given site then experience a time-varying local internal field $H_{loc}(t)$ due to the spin fluctuations of the neighboring 4f moments. The field-dependent data are also important in obtaining information on the spin-spin dynamical autocorrelation function, $q(t) = \langle S_i(t).S_i(0)\rangle$. For a spin-glass system, $q(t)$ is theoretically predicted to exhibit a power law such as $q(t) = c\ t^{-\alpha}$ or a stretched exponential $q(t) = c\ \exp\ [-(\lambda_s t)^{\beta s}]$ behavior. The subscript "s" indicates that these variables refer to the spin-spin autocorrelation function and should not be confused with the ones used in the muon relaxation

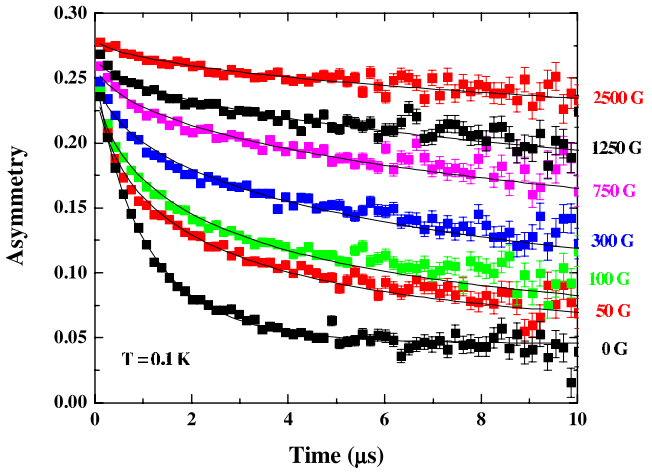

FIG. 7. (Color online) LF dependence of μSR spectra at 0.1 K. The solid line represents the fit (see text).

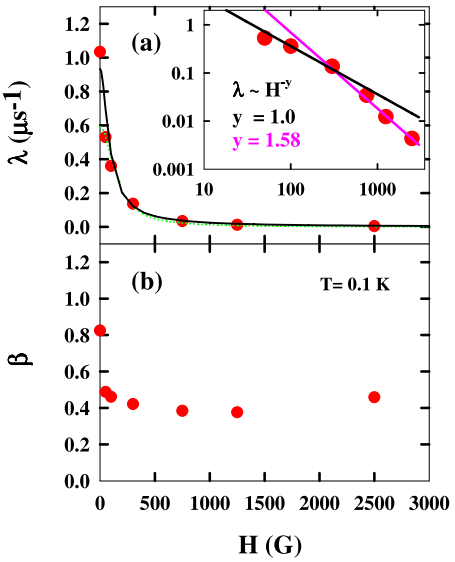

FIG. 8. (Color online) (a) LF dependence of the depolarization rate (λ) and (b) LF dependence of the exponent (β) at 0.1 K. The dotted and solid lines indicate the fit results obtained with and without taking the ZF data into account, respectively (see text). The inset shows the log-log plot with the solid lines representing power-law behaviors for different exponents.

function.[51] As shown by Keren *et al.*[51] for spin-glass systems and MacLaughlin *et al.*[41] for NFL systems, the spatially averaged muon spin relaxation function $P_z(t,H)$ at time t and longitudinal field H obeys the time-field scaling relation, $P_z(t,H)=P_z(t/H^y)$, for both the power-law and stretched exponential forms of $q(t)$. The time-field scaling has been observed for both classical spin-glass systems and NFL systems having local f moments so that the observation of the time-field scaling can be interpreted as a signature of slow spin dynamics. This scaling can, in principle, appear near any critical point but is usually associated with spin-glass-like behavior.[41] For the systems exhibiting NFL behavior, the glassy spin dynamics may arise from the effect of disorder on quantum critical fluctuations. From the observation of the time-field scaling, it is possible to obtain independent information on the nature of the spin autocorrelation function, $q(t)$: $y=1-\alpha<1$ for power-law correlation and $y=1+\beta_s>1$ for stretched exponential correlation, as long as the muon Larmor frequency $\omega_\mu=\gamma_\mu H$ is much greater than λ. It is also to be noted that the power law and stretched exponential forms mentioned here are for $q(t)$, and the same form cannot be necessarily applied to the muon spin relaxation function, $P_z(t)$.

In the following, the field dependence of the muon spin relaxation measured on $CePd_{0.15}Rh_{0.85}$ at 0.1 K is discussed. Figure 7 shows the field dependence of the μSR spectra, $P_z(t,H)$, at 0.1 K between 0 and 2500 G. With increasing field the relaxation rate initially decreases fast between zero and 50 G. Above 50 G, the rate decreases more gradually with increasing applied fields. However, there is no clear sign of a static nuclear component, i.e., a KT component, as mentioned previously in our ZF-field data. Thus we attribute this initial decrease of the relaxation rate with applied fields to the initial decoupling of the muons spin from the electronic or dynamic moments. Furthermore, the gradual decrease of the electronic damping with field may indicate that the electronic component is distributed over a wide field range. A very similar field dependence of μSR spectra has been observed in NFL systems such as $UCu_{3.5}Pd_{1.5}$, UCu_4Pd, and $CePtSi_{0.9}Ge_{0.1}$ at 50 mK.[40,41] In these systems the observed wide distribution of the muon relaxation rates at low fields has been attributed to slow or glassy dynamics associated with quantum spin-glass behavior (i.e., $T_G=0$) rather than quantum criticality such as in a uniform system. It should be noted that the value of β for $CePd_{0.15}Rh_{0.85}$ at 0.1 K exhibits a large change between 0 and 50 G applied field [see Fig. 8(b)], which could be due to the way the low applied field affects the spin dynamics of the Ce ions whose T_K is suppressed to 0 K. At present there is only one data point below 50 G that does not allow us to make any firm statement on the origin of this behavior.

The field dependence of the μSR spectra of $CePd_{0.15}Rh_{0.85}$ between 0 and 2500 G at 0.1 K is well described by the stretched exponential function, as used for the ZF data. During the fits of these data, we have kept the values of A_{BG} and A_0 fixed, as obtained from the fit of the 0.1 K ZF data. This method gave very good fits to all field data and the quality of the fit can be seen by the solid line in Fig. 7. The value of λ and β obtained from the fits are plotted as a function of field in Figs. 8(a) and 8(b). As can be seen in the figures, λ exhibits a dramatic decrease with increasing field while β exhibits a sharp drop from 0.82 to 0.52 at 50 G before it remains nearly constant up to 2500 G. In order to illustrate the behavior of λ with H, we have plotted λ versus H on a log-log scale in the inset of Fig. 8(a). From this analysis a power-law behavior, $\lambda\sim H^{-y}$, is found with $y\sim 1$ in the low-field regime and $y\sim 1.58$ in the high-field regime. It is interesting to compare these values with $y=1.6$ observed for $CePtSi_{0.9}Ge_{0.1}$ at 50 mK between 50 and 1000 G, and $y=1.0$ observed for $YbRh_2Si_2$ at 20 mK between 10 and 400 G.[41,42] On the other hand, $CeRu_4Sn_6$, exhibiting NFL behavior with a spin gap, has a very small value of $y=0.17$.[44] It is to be noted that we also tried to fit the longitudinal-field data by keeping (i) β, A_{BG}, and A_0 fixed, and (ii) β and A_{BG} fixed

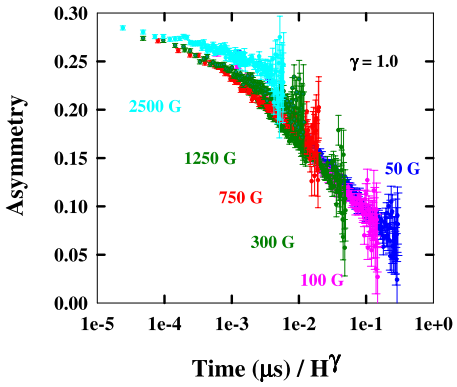

FIG. 9. (Color online) Time-field scaling of the μSR relaxation function, $P_z(t)$ versus (t/H^y), for $CePd_{0.15}Rh_{0.85}$ at 0.1 K.

to the ZF values at 0.1 K. However these constraints did not yield good fitting results, indicating that the observed field dependence of β in Fig. 8(b) is an intrinsic property of $CePd_{0.15}Rh_{0.85}$, i.e., it is not due to an artifact arising from the fitting procedure.

Another method of analyzing the longitudinal-field data at fixed temperature is to use a time-field scaling plot. Considering the observation of the time-field scaling in $UCu_{5-x}Pd_x$ ($x=1$ and 1.50), $CePtSi_{1-x}Ge_x$,[40,41] as well as of the spin-glass system AgMn (0.5 at %) above T_g,[49] we have plotted the relaxation function $P_z(t,H)$ against the scaling variable (t/H^y) for $CePd_{0.15}Rh_{0.85}$ between 0 and 2500 G at 0.1 K in Fig. 9. In order to obtain the best scaling plot, we have varied the value of y in steps of 0.1 between 0.5 and 3.0. The best scaling of the overall data can be obtained with $y=1.0\pm0.1$, except for the high-field data with 2500 G field, which show considerable deviation from the scaling curve (see Fig. 9). The deviation of the high-field data from the scaling curve was also observed for $UCu_{3.5}Pd_{1.5}$ and UCu_4Pd, in which the latter exhibits considerable deviation compared with the former. The observed scaling exponent $y=1.0$ for $CePd_{0.15}Rh_{0.85}$ is higher than the values observed for $UCu_{3.5}Pd_{1.5}$ ($y=0.7$) and UCu_4Pd ($y=0.35$) but smaller than the $y=1.6$ observed for $CePtSi_{1-x}Ge_x$ ($x=0$ and 0.1). The observed scaling exponent of $y\sim1$ for $CePd_{0.15}Rh_{0.85}$ may suggest that $q(t)$ can be well approximated by either a power-law or a stretched exponential form. It should also be noted that we did not use any specific information on the form of $P_z(t)$ in obtaining the form of $q(t)$. It would be interesting to investigate directly the form of $q(t)$ using a neutron spin-echo technique for $CePd_{0.15}Rh_{0.85}$.

Now let us discuss the spin autocorrelation time τ_c that can be estimated from the longitudinal-field dependence of λ as follows:

$$\lambda = (2\gamma_\mu^2\langle H_{\rm loc}^2\rangle\tau_c)/[1+(\gamma_\mu^2 H_{\rm app}^2\tau_c^2)^p], \tag{6}$$

where $\langle H_{\rm loc}^2\rangle$ is the second moment of the field distribution at the muon stopping sites. τ_c is related to the imaginary component of the q-independent dynamical susceptibility, $\chi''(\omega)$, through the fluctuation-dissipation theorem[55]

$$\tau_c = (k_B T/\mu_B^2)[\chi''(\omega)/\omega] \tag{7}$$

for $\hbar\omega \ll k_B T$. We fitted the field dependence of λ in Fig. 8(a) using Eq. (6) first by keeping $p=1$, which yields a good fit to all the data except for the ZF-field point [see the dotted line in Fig. 8(a)], with the parameter values $(\gamma_\mu^2\langle H_{\rm loc}^2\rangle)=1.97$(MHz) and $\tau_c=8\times10^{-8}$ s. This type of behavior has also been observed for several heavy fermion compounds with NFL-like behavior in their bulk properties: $CeCoGe_{1.8}Si_{1.2}$ with $\tau_c=4\times10^{-8}$ s,[48] $Ce_{0.7}Th_{0.3}RhSb$ with $\tau_c=5.8\times10^{-8}$ s,[56] $CeInPt_4$ with $\tau_c=3.7\times10^{-9}$ s,[57] Ce_7Ni_3 with $\tau_c=4.7\times10^{-9}$ s,[58] $CeRu_4Sb_{12}$ with $\tau_c=9.4\times10^{-9}$ s,[56] and $CeRu_4Sn_6$ with $\tau_c=2.3\times10^{-8}$ s.[44] Variation of the parameter p provides the best fits to all the data including the ZF point [see the solid line in Fig. 8(a)] with the parameter values of $(\gamma_m^2\langle H_{\rm loc}^2\rangle)=1.64$(MHz), $\tau_c=17\times10^{-8}$ s, and $p=0.67$. At present, we cannot provide good justifications for the use of parameter p other than that we choose this particular value in order to obtain a good fit to the ZF-data point. It is to be noted that the good fit to $\lambda(H)$ was obtained for both $Ce_{0.7}Th_{0.3}RhSb$ and $CeRu_4Sn_6$ with $p=0.338$ and 0.221, respectively, in Eq. (6). The observed value of τ_c in $CePd_{0.15}Rh_{0.85}$ and in $CeCoGe_{1.8}Si_{1.2}$, as well as in $Ce_{0.7}Th_{0.3}RhSb$, is much larger than that of 10^{-10}–10^{-11} s observed in the metallic spin-glass systems, e.g., CuMn with 5 at. % of Mn,[53] but also larger than that in ordered systems such as Ce_7Ni_3, $CeInPt_4$, and $CeRu_4Sb_{12}$. The observed large value of τ_c in $CePd_{0.15}Rh_{0.85}$ may originate from disordered spin-spin correlations and can yield very slow or glass-type spin dynamics at low temperatures.[40,41] On the other hand, the observed high value of τ_c in ordered $CeRu_4Sn_6$ was explained in terms of a very high residual resistivity (550 $\mu\Omega$ cm), which indicates some sort of site disorder or vacancies.[59]

3. Comparison with other NFL systems

It is important for us to compare the μSR results of $CePd_{0.15}Rh_{0.85}$, which exhibits NFL behavior near the FM-QCP, with those of other systems exhibiting NFL behavior. For this purpose, we have plotted $P_z(t)$ versus time for several NFL systems of stoichiometric compounds without doping, as well as of chemically substituted alloys in Fig. 10. We chose stoichiometric compounds, which exhibit interesting NFL behavior, for comparison. For example, $CeRu_4Sn_6$ and $CeRu_4Sb_{12}$ exhibit NFL behavior with a spin gap formation in the density of states near the Fermi level. Despite the spin gap, the low-temperature heat capacity of these compounds is very large: $\gamma_{\rm ele}=0.4$ J/mole-K^2 at 0.2 K and 0.4 J/mole-K^2 at 0.12 K, respectively, and they exhibit logarithmic behavior in the C/T plot.[59,60] We note that the origin of the high value of C/T in the presence of a spin gap is still under discussion. On the other hand, $CeNi_9Ge_4$ shows unusual NFL behavior: the heat capacity exhibits NFL behavior $C/T\sim\ln(T)$, $\gamma_{\rm ele}=5.5$ J/mole-K^2 at 0.08 K,[61] but the low-temperature susceptibility shows FL-type behavior, a constant value at low temperature. Furthermore, $CeRh_{0.8}Pd_{0.2}Sb$ exhibits NFL behavior near an antiferromagnetic quantum phase transition,[62] $\gamma_{\rm ele}=0.58$ J/mole-K^2 at 1.5 K, while from the heat capacity it has been shown that the NFL behavior in

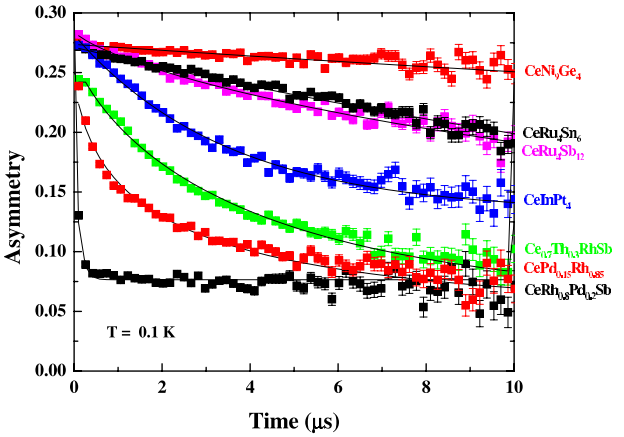

FIG. 10. (Color online) LF-μSR spectra of various non-Fermi-liquid systems at low temperatures in applied fields of 50 G. $CeNi_9Ge_4$ (Michor *et al.*, unpublished), $CeRu_4Sn_6$ (Strydom *et al.*, Ref. 44), $CeRh_{0.8}Pd_{0.2}Sb$ (Adroja *et al.*, Ref. 67), and $Ce_{0.7}Th_{0.3}RhSb$ (So *et al.*, unpublished).

$Ce_{0.7}Th_{0.3}RhSb$, $\gamma_{ele}=0.6$ J/mole-K^2 at 0.05 K, is possibly due to the Griffiths phase formation.[2,63] It is obvious from Fig. 10 that the stoichiometric compounds exhibit smaller relaxation rates compared with those observed in the chemically substituted alloys. Furthermore, the strongest observed relaxation rate in $CeRh_{0.8}Pd_{0.2}Sb$ may not be entirely due to site disorder as it shows two well-defined crystal-field excitations in our inelastic neutron-scattering data.[64] After having considered all the data shown in Fig. 10, we propose that it may instead arise due to a complex antiferromagnetic ground state at $T\rightarrow 0$ K. The present comparison does not give any clear relation between γ_{ele} and the muon relaxation rate, which is in agreement with the previous comparison made by MacLaughlin *et al.*[41] for another set of ordered NFL compounds with the chemically substituted $UCu_{5-x}Pd_x$ ($x=1$ and 1.5) alloys. Furthermore, MacLaughlin *et al.*[41] have found a correlation between the normalized muon relaxation rates (or the value of stretched exponent, β), λV_{mol}^2, where V_{mol} is the volume of unit cell per formula unit and residual resistivity, $\rho(0)$. Although there are few reports on the residual resistivity of $CePd_{0.15}Rh_{0.85}$, the magnetic scattering resistivity reported by Sereni *et al.* ($\Delta\rho\sim 38$ $\mu\Omega$ cm at 6 K) (Ref. 65), as well as an estimation of the residual resistivity [$\rho(0)\sim 60-80$ $\mu\Omega$ cm] in single crystals,[66] which is inevitably sample dependent, can be taken as an upper limit of $\rho(0)\sim 80$ $\mu\Omega$ cm of $CePd_{0.15}Rh_{0.85}$. When the value of $\beta=0.833$ at 68 mK and the normalized relaxation rate, $\lambda V_{mol}^2\sim 2.314\times 10^3$ Å^6 μs^{-1} (where $\lambda=1.137$ μs^{-1} at 60 mK and $V_{mol}=45.117$ Å^3 at 300 K) were added in Fig. 15 of Ref. 41 [λV_{mol}^2 (or β) vs $\rho(0)$ plot], β of $CePd_{0.15}Rh_{0.85}$ indeed follows the trend given in Ref. 41. However the λV_{mol}^2 does show a considerable deviation from the trend given in Ref. 41. In order to follow the behavior as shown in Ref. 41 between λV_{mol}^2 and $\rho(0)$, the value of $\rho(0)$ for $CePd_{0.15}Rh_{0.85}$ should have been ~ 200 $\mu\Omega$ cm, which is not the case.

IV. CONCLUSIONS

In addition to magnetization measurements, we have used ZF- and LF-muon spin relaxation techniques between 60 mK and 4 K to investigate the low-energy spin dynamics of $CePd_{0.15}Rh_{0.85}$, which exhibits non-Fermi-liquid behavior near the ferromagnetic quantum critical point. The ZF-μSR data reveal a considerable slowing down of spin fluctuations at low temperatures, particularly below 1 K, without loss of noticeable initial asymmetry, implying the absence of static magnetic ordering. The temperature dependence of the ZF-μSR spin relaxation rate exhibits a power-law behavior, $\lambda\sim T^{-n}$, with an exponent $n\sim 0.8$, which is in good agreement with exponents ~ 0.6 obtained from power-law behavior of the temperature dependence of the dc susceptibility, as well as the exponent value ~ 0.6 in the E/T scaling of the dynamic susceptibility. The ZF data do not reveal a clear sign of diluted spin glass or classical spin–glass-type behavior down to 60 mK that would have given a peak in $\lambda(T)$ at the spin-glass temperature if it exists above 60 mK. Furthermore, the LF-μSR data at 0.1 K exhibit a time-field scaling with the exponent $y=1.0$, which may suggest that the spin-spin autocorrelation (not to be confused with the muon relaxation function) can have either a power-law or stretched exponential behavior. The observation of time-field scaling indicates that the local spin dynamics are characterized by a power-law dynamical susceptibility at low frequencies. The observed large value of the spin autocorrelation time τ_c in $CePd_{0.15}Rh_{0.85}$, even larger than that for spin-glass systems, may suggest that the disorder effect plays a role in the origin of NFL behavior. This is in agreement with the conclusions obtained from the magnetic entropy and the concentration of unscreened magnetic moments, which reveals a broad distribution of local Kondo temperatures in $CePd_{0.15}Rh_{0.85}$.[26]

ACKNOWLEDGMENTS

We wish to thank D. MacLaughlin, A. Keren, V. Krishnamurthy, P. Schlottmann, A. Schofield, and O. O. Bernal for fruitful discussions on this topic. We are grateful to J.-Y. So, H. Michor, and A. Strydom for allowing us to show their μSR data for the comparison. D.T.A. would like to acknowledge financial support from the COST-P16 program. Work at Sungkyunkwan University was supported by the CSCMR and the 21st Century Frontier R&D Program for Hydrogen Energy.

*Corresponding author. FAX: +44-1235-445720; d.t.adroja@rl.ac.uk

[1] L. D. Landau, Sov. Phys. JETP **3**, 920 (1957).
[2] G. R. Stewart, Rev. Mod. Phys. **73**, 797 (2001).
[3] P. Coleman, arXiv:cond-mat/0612006 (unpublished).
[4] H. V. Löhneysen, A. Rosch, M. Vojta, and P. Wölfle, Rev. Mod. Phys. **79**, 1015 (2007).
[5] M. B. Maple, C. L. Seaman, D. A. Gajewski, Y. Dalichaouch, V. B. Barbetts, M. C. deAndrade, H. A. Mook, H. G. Lukefahr, O. O. Bernal, and D. E. MacLaughlin, J. Low Temp. Phys. **95**, 225 (1994).
[6] J. A. Hertz, Phys. Rev. B **14**, 1165 (1976).
[7] T. Moriya, *Spin Fluctuations in Itinerant Electron Magnetism* (Springer, Berlin, 1985); G. G. Lonzarich, in *The Electron*, edited by M. Springford (Cambridge University Press, Cambridge, 1997), Chap. 6.
[8] A. J. Millis, Phys. Rev. B **48**, 7183 (1993).
[9] M. A. Continentino, Z. Phys. B: Condens. Matter **101**, 197 (1996).
[10] E. Miranda, V. Dobrosavljevic, and G. Kotliar, Phys. Rev. Lett. **78**, 290 (1997).
[11] A. H. Castro Neto, G. Castilla, and B. A. Jones, Phys. Rev. Lett. **81**, 3531 (1998).
[12] P. Coleman, Physica B (Amsterdam) **259-261**, 353 (1999); P. Coleman, C. Pépin, Q. Si, and R. Ramazashvili, J. Phys.: Condens. Matter **13**, R723 (2001).
[13] Q. Si, S. Rabello, K. Ingersent, and J. L. Smith, Nature (London) **413**, 804 (2001); Phys. Rev. B **68**, 115103 (2003).
[14] M. Nicklas, M. Brando, G. Knebel, F. Mayr, W. Trinkl, and A. Loidl, Phys. Rev. Lett. **82**, 4268 (1999).
[15] S. R. Julian, F. V. Carter, F. M. Grosche, R. K. W. Haselwimmer, S. J. Lister, N. D. Mathur, G. J. McMullan, C. Pfleiderer, S. S. Saxena, I. R. Walker, N. J. W. Wilson, and G. G. Lonzarich, J. Magn. Magn. Mater. **177-181**, 265 (1998); S. R. Julian, C. Pfleiderer, F. M. Grosche, N. D. Mathur, G. J. McMullan, A. J. Diver, I. R. Walker, and G. G. Lonzarich, J. Phys.: Condens. Matter **8**, 9675 (1996).
[16] M. Lenkewitz, S. Corsépius, G.-F. v. Blanckenhagen, and G. R. Stewart Phys. Rev. B **55**, 6409 (1997).
[17] A. V. Chubukov, A. M. Finkel'stein, R. Haslinger, and D. K. Morr, Phys. Rev. Lett. **90**, 077002 (2003).
[18] H. Maebashi, K. Miyake, and C. M. Varma, Phys. Rev. Lett. **88**, 226403 (2002).
[19] T. R. Kirkpatrick, D. Belitz, T. Vojta, and R. Narayanan, Phys. Rev. Lett. **87**, 127003 (2001).
[20] D. Belitz, T. R. Kirkpatrick, and Thomas Vojta, Phys. Rev. Lett. **82**, 4707 (1999).
[21] S. S. Saxena, P. Agarwal, K. Ahilan, F. M. Grosche, R. K. W. Haselwimmer, M. J. Steiner, E. Pugh, I. R. Walker, S. R. Julian, P. Monthoux, G. G. Lonzarich, A. Huxley, I. Sheikin, D. Braithwaite, and J. Flouquet, Nature (London) **406**, 587 (2000).
[22] D. Aoki, A. Huxley, E. Ressouche, D. Braithwaite, J. Flouquet, J. P. Brison, E. Lhotel, and C. Paulsen, Nature (London) **413**, 613 (2001); F. Lévy, I. Sheikin, B. Grenier, and A. D. Huxley, Science **309**, 1343 (2005).
[23] C. Pfleiderer, G. J. McMullan, S. R. Julian, and G. G. Lonzarich, Phys. Rev. B **55**, 8330 (1997).
[24] J. G. Sereni, R. Küchler, and C. Geibel, Physica B **359**, 41 (2005); **378**, 648 (2006).
[25] A. P. Pikul, N. Caroca-Canales, M. Deppe, P. Gegenwart, J. G. Sereni, C. Geibel, and F. Seglich, J. Phys.: Condens. Matter **18**, L535 (2006).
[26] J. G. Sereni, T. Westerkamp, R. Küchler, N. Caroca-Canales, P. Gegenwart, and C. Geibel, Phys. Rev. B **75**, 024432 (2007).
[27] O. Stockert, H. v. Löhneysen, A. Rosch, N. Pyka, and M. Loewenhaupt, Phys. Rev. Lett. **80**, 5627 (1998).
[28] G. F. Chen, I. Sakamoto, S. Ohara, T. Takami, H. Ikuta, and U. Mizutani, Phys. Rev. B **69**, 014420 (2004).
[29] D. T. Adroja, J.-G. Park, Kwang-Hyun Jangb, H. C. Walker, K. A. McEwen, and T. Takabatake, J. Magn. Magn. Mater. **310**, 858 (2007).
[30] D. R. Grempel and M. J. Rozenberg, Phys. Rev. B **60**, 4702 (1999).
[31] P. Gegenwart, J. Custers, Y. Tokiwa, C. Geibel, and F. Steglich, Phys. Rev. Lett. **94**, 076402 (2005).
[32] D. T. Adroja and B. D. Rainford (unpublished).
[33] K. Ishida, K. Okamoto, Y. Kawasaki, Y. Kitaoka, O. Trovarelli, C. Geibel, and F. Steglich, Phys. Rev. Lett. **89**, 107202 (2002).
[34] A. P. Murani, A. Severing, and W. G. Marshall, Phys. Rev. B **53**, 2641 (1996); A. Severing and A. P. Murani, Physica B (Amsterdam) **163**, 699 (1990).
[35] D. T. Adroja, J.-G. Park, K. A. McEwen, N. Takeda, M. Ishikawa, and J.-Y. So, Phys. Rev. B **68**, 094425 (2003).
[36] N. Bernhoeft, J. Phys.: Condens. Matter **13**, R771 (2001).
[37] A. M. Tsvelik and M. Reizer, Phys. Rev. B **48**, 9887 (1993).
[38] B. Andraka and A. M. Tsvelik, Phys. Rev. Lett. **67**, 2886 (1991).
[39] B. Andraka and G. R. Stewart, Phys. Rev. B **47**, 3208 (1993).
[40] O. O. Bernal, D. E. MacLaughlin, H. G. Lukefahr, and B. Andraka, Phys. Rev. Lett. **75**, 2023 (1995); D. E. MacLaughlin, O. O. Bernal, R. H. Heffner, G. J. Nieuwenhuys, M. S. Rose, J. E. Sonier, B. Andraka, R. Chau, and M. B. Maple, *ibid.* **87**, 066402 (2001); The detailed functional form of Kubo-Toyabe (KT) function is given by R. S. Hayano, Y. J. Uemura, J. Imazato, N. Nishida, T. Yamazaki, and R. Kubo, Phys. Rev. B **20**, 850 (1979).
[41] D. E. MacLaughlin, R. H. Heffner, O. O. Bernal, K. Ishida, J. E. Sonier, G. J. Nieuwenhuys, M. B. Maple, and G. R. Stewart, J. Phys.: Condens. Matter **16**, S4479 (2004).
[42] K. Ishida, D. E. MacLaughlin, K. Okamoto, Y. Kawasaki, Y. Kitaoka, G. J. Nieuwenhuys, O. O. Bernal, A. Koda, W. Higemoto, R. Kadono, C. Geibel, and F. Steglich, Physica B (Amsterdam) **329-333**, 589 (2003).
[43] H. Michor, D. T. Adroja, E. Bauer, R. Bewley, D. Dobozanov, A. D. Hillier, G. Hilscher, U. Killer, M. Koza, S. Manalo, P. Manuel, M. Reissner, P. Rogl, M. Rotter, and E.-W. Scheidt, Physica B (Amsterdam) **378-380**, 640 (2006).
[44] A. Strydom, A. D. Hillier, D. T. Adroja, S. Paschen, and S. F. Steglich, J. Magn. Magn. Mater. **310**, 377 (2007); A. Strydom, A. D. Hillier, and D. T. Adroja (unpublished).
[45] D. T. Adroja, A. D. Hillier, J.-G. Park, K. A. McEwen, and N. Takeda, ISIS Experimental Report No. RB15362, 2005 (unpublished).
[46] I. A. Campbell, A. Amato, F. N. Gygax, D. Herlach, A. Schenck, R. Cywinski, and S. H. Kilcoyne, Phys. Rev. Lett. **72**, 1291 (1994).
[47] Y. J. Uemura, T. Yamazaki, D. R. Harshman, M. Senba, and E. J. Ansaldo, Phys. Rev. B **31**, 546 (1985).
[48] V. V. Krishnamurthy, K. Nagamine, I. Watanabe, K. Nishiyama, S. Ohira, M. Ishikawa, D. H. Eom, T. Ishikawa, and T. M. Briere, Phys. Rev. Lett. **88**, 046402 (2002).

[49] K. Emmerich, F. N. Gygax, A. Hintermann, H. Pinkvos, A. Schenck, Ch. Schwink, and W. Studer, J. Magn. Magn. Mater. **31-34**, 1361 (1983).
[50] R. Cywinski and B. D. Rainford, Hyperfine Interact. **85**, 215 (1994).
[51] A. Keren, P. Mendels, I. A. Campbell, and J. Lord, Phys. Rev. Lett. **77**, 1386 (1996).
[52] S. K. Kilcoyne and R. Cywinski, J. Magn. Magn. Mater. **104-107**, 1959 (1992).
[53] Y. J. Uemura, T. Yamazaki, D. R. Harshman, M. Senba, and E. J. Ansaldo, Phys. Rev. B **31**, 546 (1985).
[54] S. W. Lovesey, A. Cuccoli, and V. Tognetti, Hyperfine Interact. **64**, 321 (1991).
[55] J. S. Toll, Phys. Rev. **104**, 1760 (1956).
[56] D. T. Adroja, A. D. Hillier, K. A. McEwen, N. Takeda, and J.-G. Park (unpublished).
[57] A. D. Hillier, D. T. Adroja, S. R. Giblin, W. Kockelmann, B. D. Rainford, and S. K. Malik, Phys. Rev. B **76**, 174439 (2007).
[58] A. Schenck, F. N. Gygax, K. Umeo, T. Takabatake, and D. Andreica, J. Phys.: Condens. Matter **18**, 1955 (2006).
[59] I. Das and E. V. Sampathkumaran, Phys. Rev. B **46**, 4250 (1992); A. M. Strydom, Z. Guoa, S. Paschen, R. Viennois, and F. Steglich, Physica B (Amsterdam) **359-361**, 293 (2005).
[60] N. Takeda and M. Ishikawa, J. Phys. Soc. Jpn. **69**, 868 (2000); Physica B **281**, 388 (1999); J. Phys.: Condens. Matter **13**, 5971 (2001).
[61] H. Michor, S. Manalo, A. D. Hillier, D. T. Adroja, E. Bauer, G. Hilscher, U. Killer, P. Rogl, and M. Rotter (unpublished).
[62] L. Menon, F. E. Kayzel, A. de Visser, and S. K. Malik, Phys. Rev. B **58**, 85 (1998).
[63] J. S. Kim, E. W. Scheidt, D. Mixson, B. Andraka, and G. R. Stewart, Phys. Rev. B **67**, 184401 (2003).
[64] J.-G. Park, D. T. Adroja, K. A. McEwen, and A. P. Murani, J. Phys.: Condens. Matter **14**, 3865 (2002).
[65] J. G. Sereni, E. Beaurepaire, and J. P. Kappler, Phys. Rev. B **48**, 3747 (1993).
[66] C. Geibel (private communication).
[67] D. T. Adroja, J.-Y. So, J.-G. Park, K. A. McEwen, and A. D. Hillier, ISIS Experimental Report No. RB13064, 2002 (unpublished); D. T. Adroja, A. D. Hillier, J.-G. Park, and K. A. McEwen (unpublished).